# Tailorable electromagnetic interference shielding using nickel coated glass fabric-epoxy composite with excellent mechanical property

M. Angappan[a,b], Pritom J. Bora[c], K.J. Vinoy[d], Praveen C. Ramamurthy[b,c,*], K. Vijayaraju[a]

[a] Aeronautical Development Agency, Indian Institute of Science, PB No 1718, Bengaluru 560012, India
[b] Department of Materials Engineering, Indian Institute of Science, Bengaluru 560012, India
[c] Interdisciplinary Centre for Energy Research (ICER), Indian Institute of Science, Bengaluru 560012, India
[d] Department of Electrical and Communication Engineering, Indian Institute of Science, Bengaluru 560012, India

## ABSTRACT

Glass fibre fabric was coated with nickel using electroless plating technique. A suitable pre-treatment method was adopted to make the glass fabric surface catalytic. The glass fabric was coated to various thicknesses of nickel by varying the plating parameters. The effect of coating thickness on electromagnetic interference (EMI) shielding and absorption was studied in J (5.8–8.2 GHz), X (8.2–12.4 GHz) and Ku-(12.4–18 GHz) bands. The optimum coating thickness of 400 nm would be desirable to achieve shielding effectiveness of 30 dB in J, X and Ku-band (efficiency level of 99.9%). The absorption co-efficient was found to be dominant for coating thickness of ~ 32 nm. Further, a 3 mm thick epoxy-glass laminate was made by embedding a single layer of nickel coated glass fibre fabric with a coating thickness of ~ 6 μm. It was observed that in such a composite laminate with Ni coated fabric, EMI SE of ~ 50 dB could be achieved. It was also observed that the mechanical properties of the laminate bearing a Ni coated layer is better than the plain laminate as a result of improved interfacial characteristics in the presence of active Ni.

## 1. Introduction

Electromagnetic interference (EMI) has been identified as one of the major undesirable effects on the performance of modern avionics equipment [1–3]. In order to mitigate EMI, several shielding techniques are employed and, in particular, the use of shielding materials has been observed to be most promising [1–3]. Traditionally, use of metallic alloys of copper or nickel or stainless steel has been the preferred choice [4]. However, due to their higher density, specific shielding efficiency is low and therefore recent focus has shifted to light weight shielding materials which can operate on a broad frequency bandwidth [1,2]. For non structural applications, metal coated polymers are often employed to protect against EMI [2,4]. The approach, in the recent past, has gradually shifted towards the modification of the polymer itself with the introduction of conductive fillers into them [3,4]. Several metallic fillers such as stainless steel fibers and metal coated fillers, like nickel coated carbon fibers are embedded in the polymer matrix [4]. Carbon based materials for EMI shielding has also been identified as an alternate by various research groups [4–8]. Carbon nanotubes and graphene have been used as conductive fillers due to their high electrical conductivity, excellent mechanical properties, light weight and large aspect ratio [5–8]. Though excellent progress has been made with filler based approach for non-structural applications, there are concerns with regard to mechanical properties when the approach is extended to structural composites [4].

In order to achieve the desired EMI shielding effectiveness (SE) in a targeted frequency range (8–18 GHz), it is required to make the composite materials to be adequately conducting [1–3]. The electrical conductivity in turn depends on the shielding thickness, frequency and filler content. EMI SE of 30 dB corresponding to 99.9% attenuation of incident EM radiation is considered adequate for most applications [1,9]. The electrical conductivity of the composites that are made using these fillers strongly depends on critical percolation threshold of filler additions [1,10]. Although higher filler content is advantageous in achieving higher shielding efficiency, the consequent mechanical properties of the composites are often compromised as a result of poor filler-matrix bonding [10–15]. The situation is not different even with the use of metal coated chopped fibres as fillers [10–14]. In the case of composites used for structural applications, compromise in mechanical properties is not acceptable.

Glass and carbon fibre reinforced polymer composites are widely used in structural applications of aircraft. Being a poor electrical conductor, glass fibre reinforced polymer (GFRP) composites will not be able to provide EMI shielding which is essential for certain applications. As outlined above, use of conductive fillers is not advisable from mechanical strength view point. Use of metal coated fabric itself is another option. While it is observed that chopped glass and carbon fibres are modified with conducting metallic coatings, there have been limited efforts on the modification of continuous reinforcement like glass fabric [4]. Present effort attempts to evaluate the EMI SE of electroless nickel

plating on woven glass fabric as a possible EMI shielding coating. The effect of coating on mechanical properties when the coated fabric is incorporated in a structural laminate along with EMI SE is also evaluated.

## 2. Experimental

### 2.1. Composite preparation

E-glass is chosen for the present study as this is widely used for fabrication of fibre reinforced composites in a few aircraft applications. E-Glass is alumino-borosilicate glass with very less alkali oxides. E-glass woven fabric layers of 200 μm thickness (with average fibre diameter of 9.5 ± 0.2 μm) were used in this study (sourced from Atul Pvt Ltd, India). Pre-treatment of non-metal substrates to make the surfaces catalytic is an important step in electroless nickel plating of non-metals. The pre-treatment [15] process followed in the current study involves a two-step process.

In the first step, the non-metal surface is treated in a sensitizing solution of 35 g of $SnCl_2$ and 50 g of HCl in 500 ml of water at room temperature for 10 minutes followed by a rinsing with DI water. In the second step, surface activation is achieved by treating the glass fabric layers in the activation solution of 250 mg of $PdCl_2$ and 3 g of HCl in 1000 ml of water at room temperature for 10 min followed by rinsing using DI water. The glass fabric layers were then immersed in the plating bath for platting. The plating bath composition is presented in Table 1. Here, nickel sulphate provides $Ni^{2+}$ ions and sodium hypophosphite acts as a reducing agent. The $Ni^{2+}$ are reduced by the free electrons released by the reducing agent. The other chemical trisodium citrate is used as complexing agent and it forms a complex with the nickel ions and controls the availability of nickel ions for the reduction reaction. Ammonium sulfate as a buffering agent controls the pH variation of the bath during reaction. The metal based stabilizing agent controls the reaction rate.

The bath was operated at 75 and 85 °C temperature with a pH of 4.5 to 5. The plating parameters for each fabric was controlled such that glass fabrics were coated to varying thicknesses. The coating thickness of the fabric was established by weight gain method and correlated using FESEM measurement. The coating thickness obtained as a function of coating temperature and duration is presented in Table 2.

Glass fibre reinforced polymer (GFRP) composite laminates were also made with and without incorporation of a nickel coated fabric layer for evaluation of both EMI SE and mechanical properties. Epoxy resin of type LY5052 and hardener CH5052 supplied by M/s Huntsman Advanced Materials (India), was used for fabrication of the laminate. The nickel coated glass fabric was kept as a middle layer during lay-up of the laminate of size 300 mm × 300 mm × 3 mm.

### 2.2. Characterizations

The samples that were drawn from coated glass fabrics were pasted onto the carbon tape and sputter coated with gold so as to examine the surface morphology by using high resolution scanning electron microscope (SEM, Carl Zeiss). The chemical composition was examined using X-ray fluorescence (XRF). The EMI SE was evaluated by using a vector network analyzer (VNA, Agilent N5230A). Rectangular waveguides

**Table 1**
Details of electroless nickel coating bath composition.

| Sl. no. | Chemicals | Composition (g/l) |
|---|---|---|
| 1 | Nickel Sulfateheptahydrate ($NiSO_4.7H_2O$) | 25–30 |
| 2 | Trisodium Citrate | 35–40 |
| 3 | Ammonium Sulfate | 10–15 |
| 4 | Sodium Hypophosphite | 20–25 |

**Table 2**
Electroless coating duration and obtained thickness.

| Serial no. | Coating parameter | | Average coating thickness (nm) |
|---|---|---|---|
| | Temperature (°C) | Duration (s) | |
| 1 | 75 | 20 | 32 ± 5 |
| 2 | | 40 | 43 ± 5 |
| 3 | | 60 | 55 ± 5 |
| 4 | 85 | 20 | 66 ± 4 |
| 5 | | 40 | 133 ± 7 |
| 6 | | 60 | 202 ± 9 |
| 7 | | 120 | 405 ± 13 |
| 8 | | 180 | 607 ± 17 |
| 9 | | 1800 | 6020 ± 20 |

WR137, WR-90 and WR-62 were used to cover measurements in the J-band (5.8–8.2 GHz), X-band (8.2–12.4 GHz) and Ku-band (12.4–18 GHz), respectively. The complete two-port calibration of the VNA (thru-reflect-line or TRL standard) was carried out before commencing the measurements. The reflection, absorption and transmission co-efficient were derived from the measured S-parameters [17].

The GFRP laminate consisting of nickel coated fabric was also characterised for EMISE. In order to examine the mechanical properties, testing for tensile strength and interlaminar shear strength (ILSS) were carried out on laminates with and without nickel coated layer. Tensile test was carried out as per ASTM D 3039 with a rate of loading of 0.5 mm /min. Test for ILSS was carried out as per ASTM 2344 with a rate of loading of 1 mm/min.

## 3. Results and discussion

Optical photographs of the E-glass fabric and Ni coated glass fabrics for varying duration were shown in Fig. 1. Fig. 2 shows the surface morphologies of Ni coated glass fabrics for varying duration along with E-glass fabric. The coating was found to be uniform. The composition of the coating was analysed using XRF and the obtained results are shown in the Table 3. The XRF results confirms the presence of Ni as a major component and P as an alloying element. Origin of Ti, Si, Al and Fe are from substrate i.e. E-glass fabric. Origin of Sn is from sensitization treatment which was used during pre-treatment. The coated and uncoated E-glass fabric were characterised by XRD analysis. As shown in Fig. 3, a broad peak was observed at 2θ = 45° along with other diffused peaks. The absence of any other characteristics peak in this pattern indicates that the coating is an alloy of Ni and P and has an amorphous structure.

The reflection (R), transmission (T) and absorption co-efficient (A) are obtained from the measured S-parameters as follows [17],

$$R = 10^{\frac{S_{11}}{10}} \tag{1}$$

$$T = 10^{\frac{S_{21}}{10}} \tag{2}$$

$$A = 1 - R - T \tag{3}$$

The obtained EMI SE of Ni coated glass fabric for various coating thicknesses in the J-band (5.8–8.2 GHz) is shown in Fig. 4(a). It was observed that EMI SE was gradually increases with an increase in coating thickness. It increased from 7 dB to 55 dB when the coating thickness was increased from ~ 32 nm to ~ 6000 nm, respectively. Similar behaviour was observed in X-band and Ku-band as well (Fig. 4(b) and (c)). It is well known that EMI shielding is the material property which depends on several factors such as frequency, conductivity, source to shield distance, thickness, dielectric loss and EM attenuation loss [17,19,21,22]. The resistivity of the coated fabric was measured using two-probe method. The resistivity of the uncoated cloth was $1 \times 10^5$ Ω-m. The resistivity was found to drop with an increase in coating thickness and attained the theoretical value of electroless Ni-P[18]
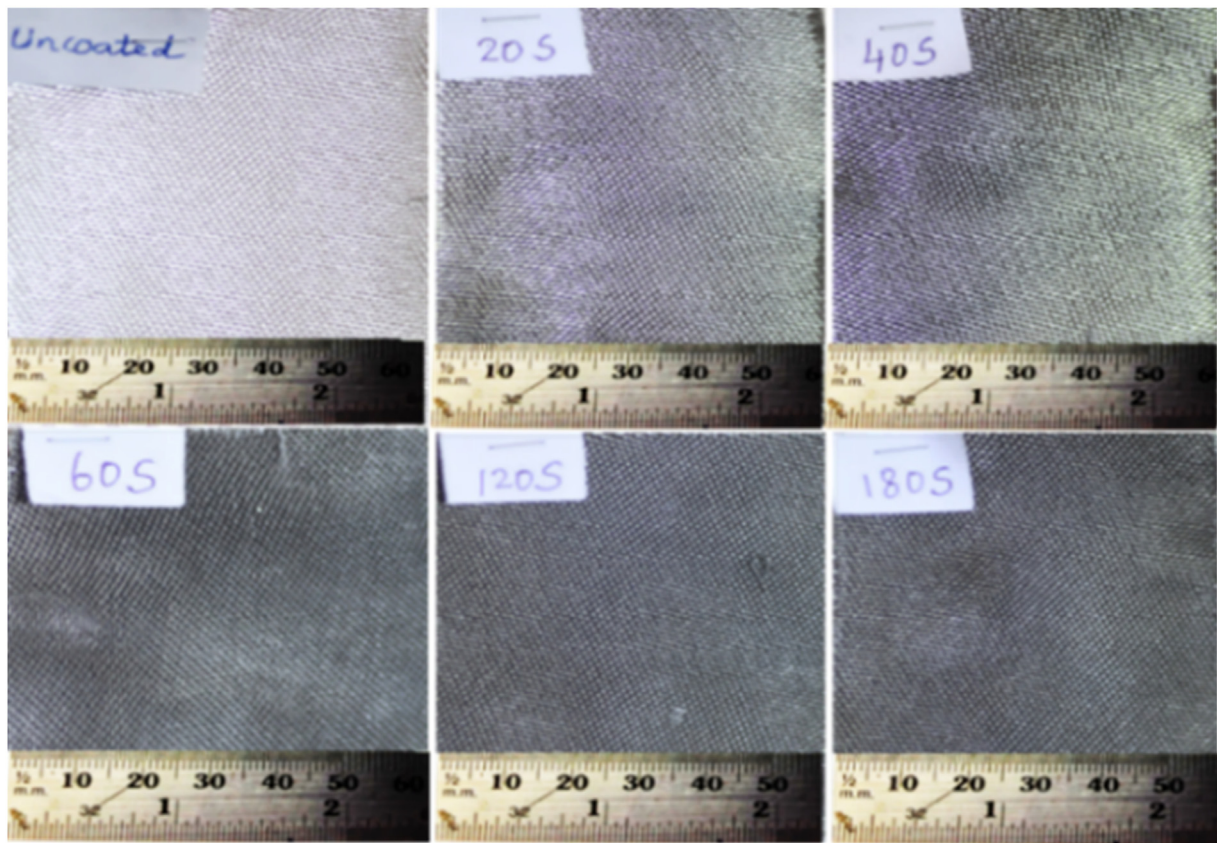
**Fig. 1.** Optical images of uncoated and Ni coated glass fabrics.

system for coating thickness of 400 nm and above. The resistivity values measured for varying coating thicknesses is presented in Table 4. It indicates the enhancement of conductivity with increasing coating thickness which results in improving the shielding effectiveness. The reflection, absorption and transmission corresponding to 11 GHz is also presented in Table 4. The transmission, reflection and absorption co-

**Table 3**
Elemental composition of Ni coated glass fabric.

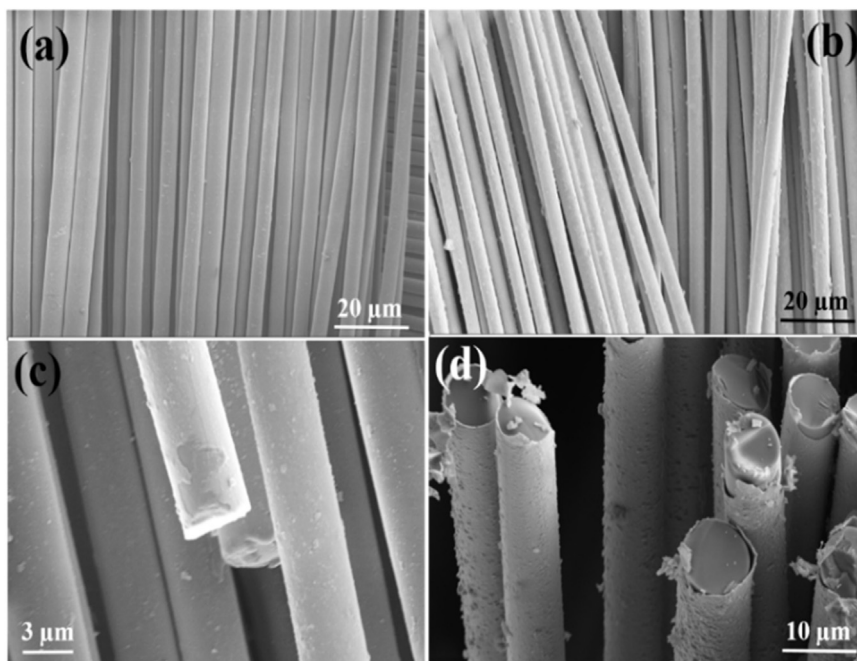| Elements | Ni | P | Si | Al | Fe | Ti | Sn |
|----------|-------|------|------|------|------|------|------|
| Wt (%) | 80.88 | 8.65 | 7.30 | 2.23 | 0.35 | 0.32 | 0.27 |



**Fig. 2.** Surface morphology of **(a)** E-glass fabric and **(b-d)** Ni-glass fabrics.
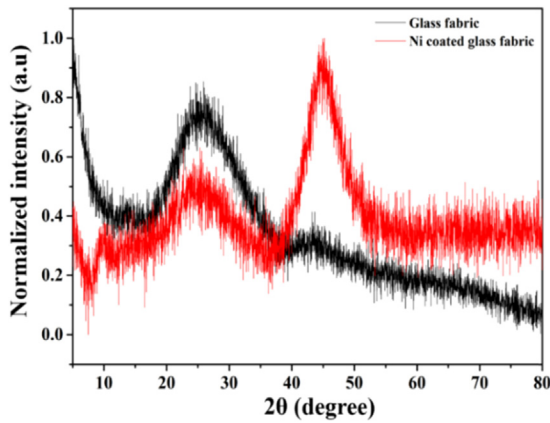
**Fig. 3.** XRD pattern of glass fabric and nickel coated glass fabrics.

**Table 4**

Variation of resistivity, absorption (A), reflection (R) and transmission (T) coefficient of Ni coated glass fabric for different coating thicknesses.

| Sl. no. | Coating thickness (NM) | Resistivity (Ω-m) | A, R & T @ 11 GHz | | |
|---------|------------------------|-------------------|-------|-------|-------|
| | | | R (%) | T (%) | A (%) |
| 1 | 32 ± 5 | 0.7E-03 | 23 | 25 | 51 |
| 2 | 43 ± 5 | 0.78E-03 | 44 | 22 | 34 |
| 3 | 55 ± 5 | 0.94E-03 | 75 | 2.5 | 22.5 |
| 4 | 66 ± 4 | 1.00E-03 | 85 | 1.65 | 13.3 |
| 5 | 133 ± 7 | 6.65E-03 | 89.4 | 0.93 | 9.67 |
| 6 | 202 ± 9 | 2.65E-03 | 92.5 | 0.276 | 7.19 |
| 7 | 405 ± 13 | 3.00E-03 | 94.9 | 0.05 | 5.01 |
| 8 | 607 ± 17 | 2.00E-06 | 95.9 | 0.02 | 4.06 |
| 9 | 6020 ± 20 | 1.00E-06 | 98.99 | 4.0 E-05 | 1 |

efficient are also shown in Fig. S1 (Supporting information) for X-band.

The reflection remaining dominant when conductivity was increased as a function of coating thickness (Table 4). However, absorption becoming dominant when coating thickness was reduced to 32 nm. For coating thickness of 32 nm, the absorbed EM energy at 11 GHz is 51% whereas 23% of energy is reflected and 25% transmitted. The dissipation of EM energy is related to the skin depth available with the conducting substrate. The depth where the incident EM energy is dissipated to 1/e of its original level is called skin depth or penetration depth [21,22] and it exists within the outer layer of the conducting surface [16,20,21]. With an increase in conductivity and frequency, expected skin depth keeps getting reduced which in turn reduces the effective cross sectional area available for electron flow [20,21]. If the coating thickness is reduced much below optimum skin depth, the consequent increase of the resistance changes the shielding

mechanism to absorption from reflection as a result of ohmic heating [20]. Hence, EMI SE is dominated by absorption at high frequency situations when the thickness is reduced. Therefore, achieving a desired conductivity level which is controlled by coating thickness is a prerequisite to achieve the targeted shielding efficiency [20]. The EMI SE of 30 dB is the adequate for achieving the shielding efficiency of 99.9% [1]. The variation of EMI SE with coating thickness was shown in the Fig. 4(d). It was established in the present study that nickel coating thickness of minimum 400 nm would be adequate so as to achieve the EMI SE above 30 dB (Fig. 4(d)). Further, minimum coating thickness (~ 30 nm) results in absorption predominant shielding (Fig. S1, Supporting information).

For practical applications, higher EMI SE is always advantageous [1–8]. As higher EMI SE (~ 55 dB) was obtained for ~ 6 μm coating thickness, it was chosen to fabricate GFRP laminate using this fabric where 6 uncoated fabric and one coated fabric in the mid-thickness were used. The same laminate was examined for mechanical properties.
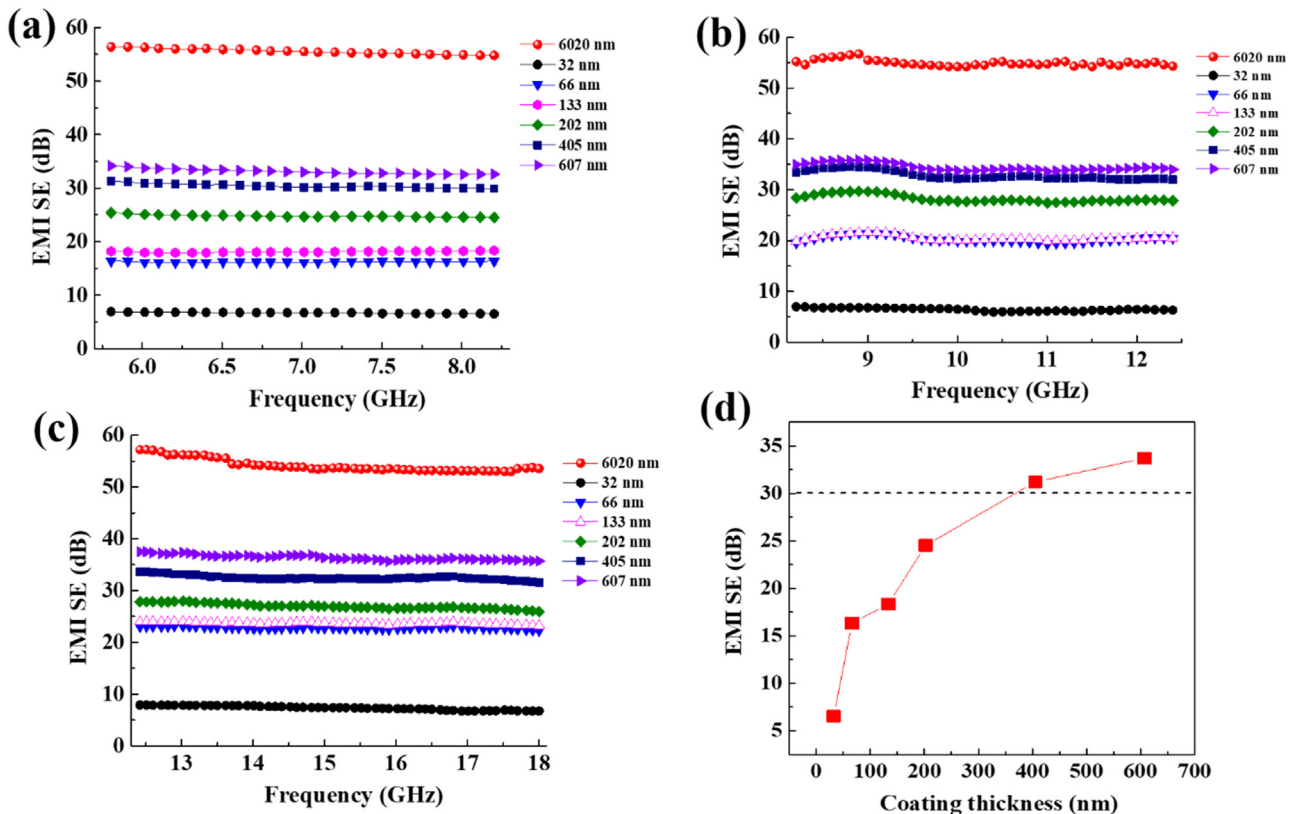


**Fig. 4.** EMI SE (dB) of Ni coated glass fabric for various coating thickness in **(a)** J-band (5.8–8.2 GHz), **(b)** X-band (8.2–12.4 GHz) and **(c)** Ku-band (12.4–18 GHz) respectively. **(d)** Variation of EMI SE with respect to coating thickness.
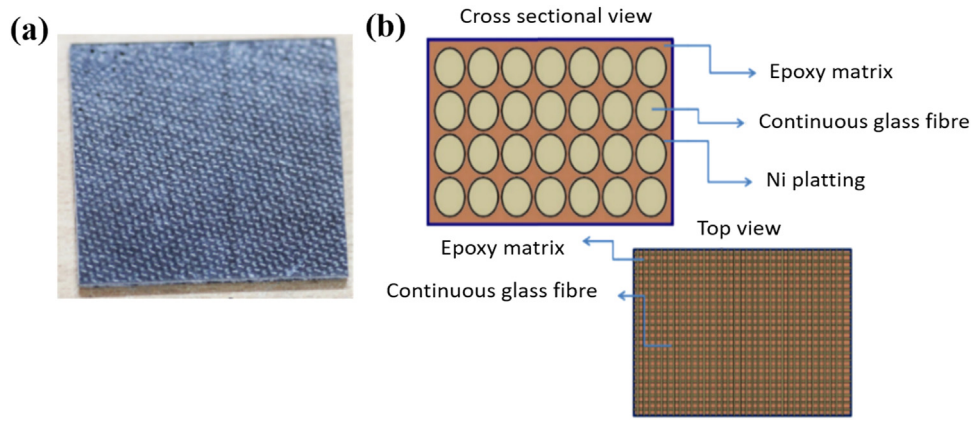
**Fig. 5.** (a) Optical image **(b)** schematic of epoxy-Ni coated glass fabric.
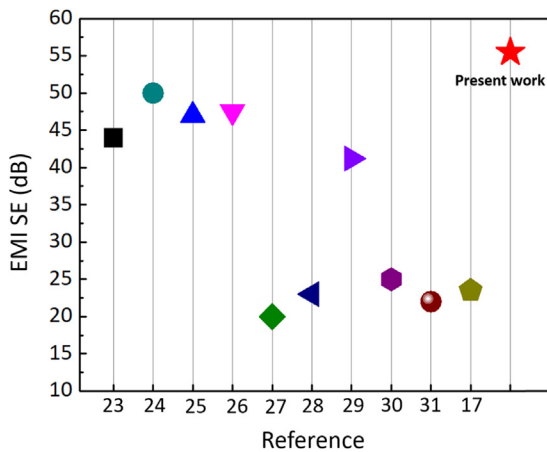


**Fig. 6.** EMI SE (dB) of various reported Ni coated based composites with present composite.

The optical and schematic structure of the prepared epoxy-Ni coated fabric composite is shown in Fig. 5(a) and (b), respectively. The epoxy-Ni coated fabric laminate also shows EMI SE ~ 55 dB.

The reported average EMI SE of different Ni based composite materials with the present material is shown in the Fig. 6. The present composite material is much superior for achieving effective EMI SE, as compared to various Ni based composites [17,23–31] in the Fig. 6.

The properties of fibre-matrix interface in terms of good interfacial bonding is important in determining the performance of the composite laminates [25]. The good interfacial bonding improves ILSS, compressive strength, strain to failure and fatigue life [25,32]. Generally, as drawn fibres will have lower interlaminar shear strength due to weak adhesion and poor bonding between the fibre and matrix. Therefore, commonly pre-treatment called 'sizing' is applied to the fibres so as to improve the bonding between the fibres and matrix [20,25,32–34]. The pre-treatment will enhance the wettability of the fibres and in turn increase the ILSS and compressive strength [32].

The ILSS of the GFRP laminate where nickel coated fabric was placed in the mid thickness was ~ 35 MPa while it was ~ 25 MPa for the plain GFRP laminate (Fig. 7(a)). It indicates that the interfacial bonding of the laminate having nickel embedded layer is better than the plain laminate. The electroless nickel plated deposits leaves an active nickel on the fabric surface which enhances the interfacial bonding with the epoxy matrix [18,32]. The tensile strength of the laminate with nickel embedded layer remains comparable with the plain GFRP laminate (Fig. 7(b)). Furthermore, laminate consisting of nickel embedded layer was found to exhibit better extension than the plain laminate.

It is shown in the present work that a free standing Ni coated glass fabric or a GFRP laminate with Ni coated layer exhibiting tailorable shielding characteristics and better mechanical properties. The nickel coated glass fabric to higher thicknesses (~ 400 nm) can be used for such applications as a stand-alone fabric or as a composite laminate. In applications such as radar barriers and artificial horizon of military hardware, shielding electromagnetic radiation predominantly by absorption is preferred and glass fabric coated to ~ 32 nm can be very useful and also for applications requiring thin film absorber [20].
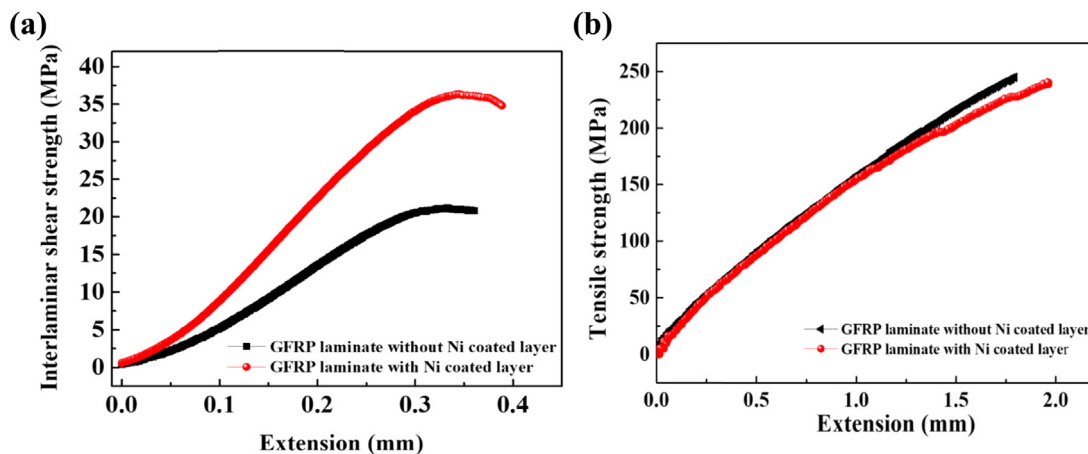


**Fig. 7.** Comparison of **(a)** interlaminar shear strength and **(b)** tensile strength of GFRP laminate with and without Ni coated layer.

## 4. Conclusions

In summary, the EMI shielding effectiveness of nickel coated glass fabric was examined as a function of coating thickness. The optimum coating thickness of 400 nm would be desirable to achieve shielding effectiveness of 30 dB in J, X and Ku-band (efficiency level of 99.9%). It was found that EMI shielding due to absorption is dominant for coating thickness of ~ 32 nm. The desired shielding efficiency was also shown by incorporating a nickel coated glass fabric into glass fibre-epoxy composite laminate. The GFRP embedded with nickel coated fabric was found to possess better mechanical properties due to its improved interfacial characteristics. The nickel coated fabric with its tailorable EM shielding characteristics and better mechanical properties can be employed for various potential applications.

## Acknowledgements

## Appendix A. Supporting information

Supplementary data associated with this article can be found in the online version at doi:10.1016/j.coco.2018.09.001

## References

[1] F. Shahzad, M. Alhabeb, C.B. Hatter, B. Anasori, S. Man Hong, C.M. Koo, Y. Gogotsi, Science 353 (2016) 1137–1140 (80-.).
[2] P.J. Bora, K.J. Vinoy, P.C. Ramamurthy, Kishore, G. Madras, Electron. Mater. Lett. 12 (2016) 603–609.
[3] D.D.L. Chung, J. Mater. Sci., 39, p. 2645.
[4] S. Geetha, K.K. Satheesh Kumar, C.R.K. Rao, M. Vijayan, D.C. Trivedi, J. Appl. Polym. Sci. 112 (2009) 2073–2086.
[5] F.J.B. Calleja, R.K. Bayer, T.A. Ezquerra, J. Mater. Sci., 23, p. 1411.
[6] Y. Yang, M.C. Guptal, K.L. Dudley, R.W. Lawrence, J. Nanosci. Nanotechnol. 7 (2007) 549.
[7] N. Li, Y. Huang, F. Du, X. He, X. Lin, H. Gao, Y. Ma, F. Li, Y. Chen, P.C. Eklund, Nano Lett. 6 (2006) 1141.
[8] Y. Huang, N. Li, Y. Ma, F. Du, F. Li, X. He, X. Lin, H. Gao, Y. Chen, Carbon 45 (2007) 1614.
[9] D. Markham, Mater. Des. 21 (1999) 45.
[10] X. Luo, D.D.L. Chung, Compos. Eng. -Part B 30 (1999) 227.
[11] P.B. Jana, A.K. Mallick, S.K. De, IEEE Trans. Electromagn. Compat. 34 (1992) 478.
[12] J. Avloni, M. Ouyang, L. Florio, A.R. Henn, A. Sparavigna, J. Thermoplast. Compos. Mater. 20 (2007) 241.
[13] D.M. Bigg Battelle, Polym. Eng. Sci. 17 (1977) 842.
[14] C.-Y. Huang, J.-F. Pai, Eur. Polym. J. 34 (1998) 261.
[15] P. Mahanthesha, C.K. Srinivasa, G.C. Mohankumar, Procedia Mater. Sci., 5, 883, 1014.
[16] L.F. Chen, C.K. Ong, C.P. Neo, V.V. Varadan, V.K. Varadan, Microwave Electronics: Measurement and Materials Characterization, John Wiley & Sons, 2004.
[17] P.J. Bora, N. Mallik, P.C. Ramamurthy, Kishore, G. Madras, Compos. Eng. -Part B 106 (2016) 224.
[18] G.O. Mallory, J.B. Hajdu, A. E, S.F. Society, Electroless Plating: Fundamentals and Applications, The Society, 1990.
[19] P.J. Bora, G. Lakhani, P.C. Ramamurthy, G. Madras, RSC Adv. 6 (2016) 79058.
[20] J.W. Gooch, J.K. Daher, Electromagnetic Shielding and Corrosion Protection for Aerospace Vehicles, Springer, New York, New York, NY, 2007.
[21] C.A. Grimes, D.M. Grimes, in: 1993 IEEE Aerospace Applications Conference, Digest, 1993, pp. 217–226.
[22] P. Saini, V. Choudhary, N. Vijayan, R.K. Kotnala, J. Phys. Chem. C 116 (2012) 13403.
[23] C.-Y. Huang, J.-F. Pai, J. Appl. Polym. Sci. 63 (1997) 115–123.
[24] C.-Y. Huang, J.-F. Pai, Eur. Polym. J. 34 (1998) 261–267.
[25] W. -Y. Chiang, Y. -S. Chiang, J. Appl. Polym. Sci. 46 (1992) 673–681.
[26] C.-Y. Huang, C.-C. Wu, Eur. Polym. J. 36 (2000) 2729–2737.
[27] K. Wenderoth, J. Petermann, K. -D. Kruse, J. -L. ter Haseborg, W. Krieger, Polym. Compos. 10 (1989) 52–56.
[28] H. Gargama, A.K. Thakur, S.K. Chaturvedi, J. Appl. Phys. 117 (2015) 224903–224909.
[29] X. Huang, B. Dai, Y. Ren, J. Xu, P. Zhu, J. Nanomater. (2015) 320306.
[30] K. Ji, H. Zhao, J. Zhang, J. Chen, Z. Dai, Appl. Surf. Sci. 311 (2014) 351–356.
[31] P.J. Bora, K.J. Vinoy, P.C. Ramamurthy, Kishore, G. Madras, Compos. Commun. 4 (2017) 37–42.
[32] S.J. Park, Y.S. Jang, K.Y. Rhee, J. Colloid Interface Sci. 245 (2002) 383–390.
[33] W.W. Wright, Mater. Des. 12 (1991) 222–227.
[34] F.X. Qin, H.X. Peng, N. Pankratov, M.H. Phan, L.V. Panina, M. Ipatov, J. Appl. Phys. 108 (2010) 044510.